Supporting Information

Programmable, Electroforming-free TiO_x/TaO_x Heterojunction-based Non-volatile Memories

*Saurabh Srivastava, Joseph Palathinkal Thomas, Kam Tong Leung**

WATLab and Department of Chemistry, University of Waterloo, 200 University Ave. W., Waterloo, ON N2L 3G1

Corresponding author email: tong@uwaterloo.ca and saurabh@smart.mit.edu

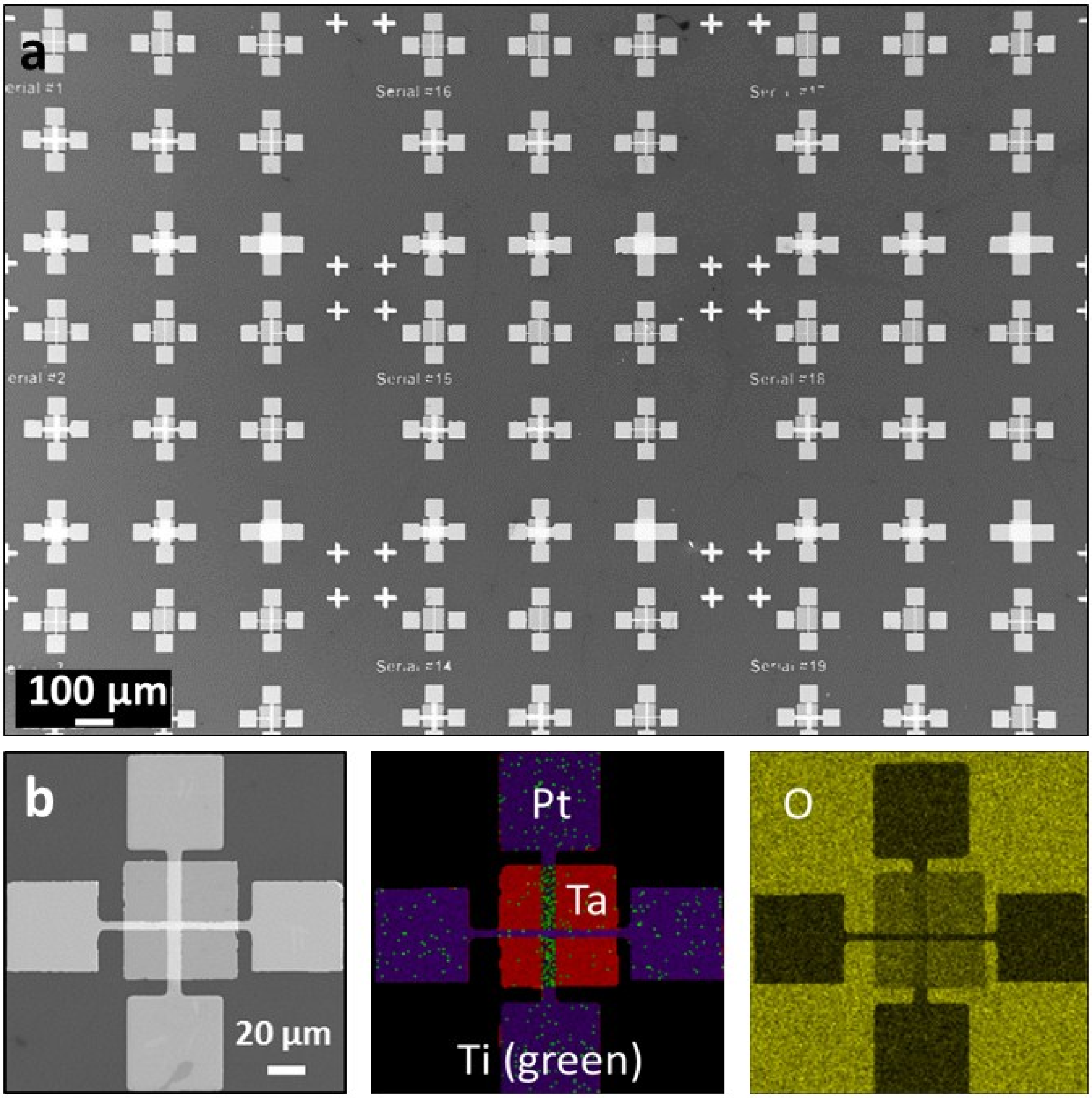

Figure S-1 | a, SEM image of arrays of memristor devices fabricated with TiO_x/TaO_x active layers of different junction sizes on a SiO_2/Si substrate. **b,** SEM image (left) and EDX elemental maps (center, right) of a typical heterojunction memristor with a 5×5 μm^2 junction size. The TiO_x layer (green) was deposited on a Pt layer (purple) as the bottom electrode (horizontal I-bar) followed by the Pt layer (purple) as the top electrode (vertical I-bar), while the TaO_x layer (red) was sandwiched between the TiO_x and the bottom electrode.

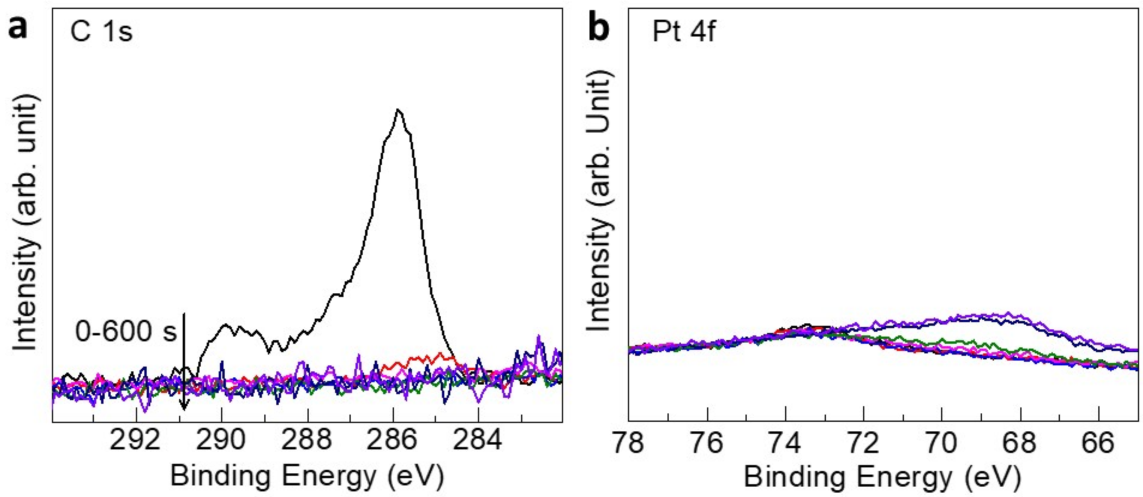

Figure S-2| Depth-profiling XPS spectra of **a,** C 1s and **b,** Pt 4f regions for the as-deposited 60-nm-thick TaO_x film on a Pt film supported on a SiO_2/Si substrate. The carbonaceous layer of the sample arising from ambient handling was removed after 5 s of sputtering, revealing a carbon free sample. The signal for Pt layer beneath the TaO_x layer is very weak because 300 s of Ar-sputtering was not sufficient to remove the TaO_x layer completely.

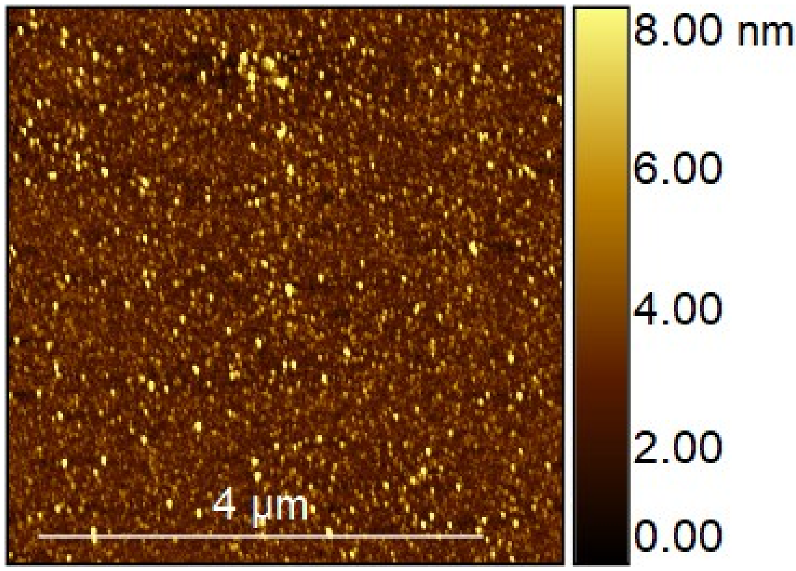

Figure S-3| AFM image of the TaO_x film to illustrate the surface roughness for a scan area of 5×5 µm^2. The roughness analysis was performed along its diagonal direction and found to be 0.84 nm RMS.

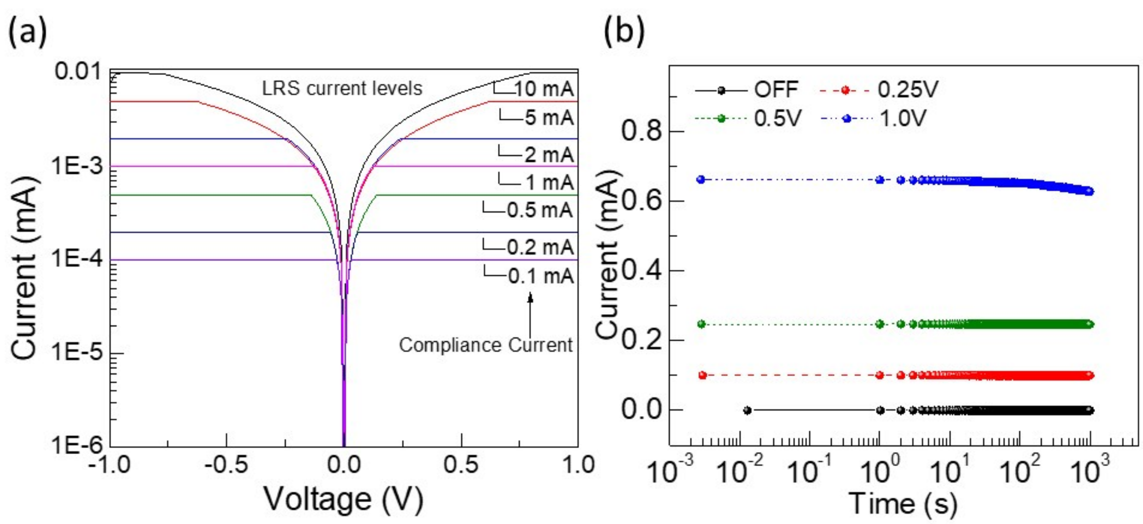

Figure S-4| a, LRS current level vs compliance current. **b,** Retention characteristics for the TiO_x/TaO_x memristor (10×10 µm^2 junction size) at different read-out voltages. For different read voltages, a very stable read current was observed even after long retention, which confirms the stability of these devices.

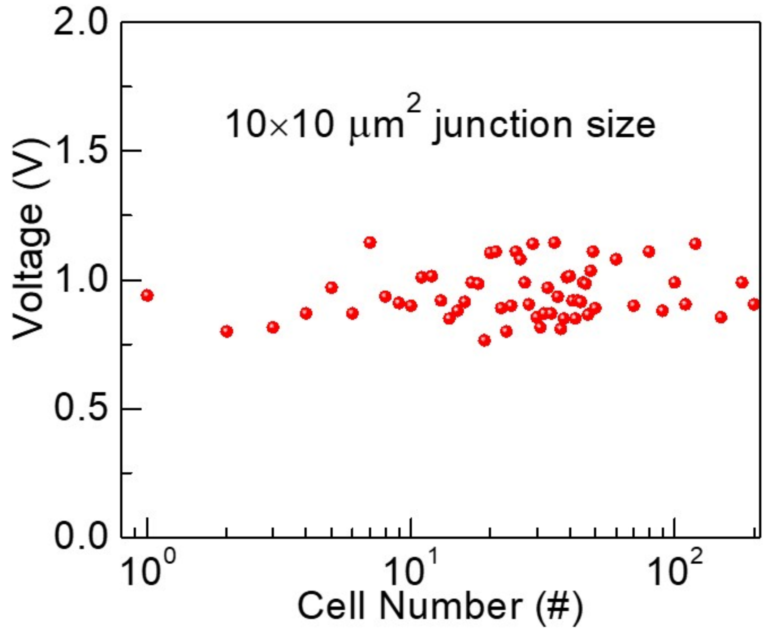

Figure S-5| SET voltages of 300 memristor devices (marked by cell number) fabricated on the same chip. The similar switching voltages of these devices show the accuracy and reproducibility of our fabrication process.

Table S1| Comparison of various memristor device architectures with single-layer and multilayer switching matrices and their respective electroforming and SET/RESET voltages. Our device out-performs all the devices based on not just single-layer switching matrices but also multilayer switching matrices. The device made by Bessonov et al. exhibits a lower SET/RESET voltage than our device but at the expense of a shorter lifetime (because of the oxidation-prone silver nanowire in ambient) along with a rather complex process.

Device Structure	**Electroforming/ Activation voltage**	**SET/RESET Voltage**	**Ref.**
Single-layer Matrix			
AFM Tip/$SrTiO_3$/Pt-Au	-5 V	±4 V	Szot et al. (2006)[1]
Pt/TiO_2/Pt	NA	2/3 V	Kwon et al. (2010) [2]
Pt/TiO_2/Pt	-6 V	±0.6	Strachan et al. (2011) [3]
Pt/Ta_2O_5/Pt	-10 V	+0.6/-0.8 V	Strachan et al. (2011) [4]
Ti-Pt/TiO_2/Au-pt	-14 V	+3/+2.5 V	Strukov et al. (2012) [5]
ZnO Nanorods	4 V	±2 V	Park et al. (2013) [6]
Pt/TiO_2/Pt	-8 V	±4 V	Jiang et al. (2013) [7]
Pt/TiO_2/Pt	Forming-free	+3.6/-4 V	Salaoru et al. (2013) [8]
Au NP/$SrTiO_3$ interface	10 V	+4/-6 V	Hou et al.(2014) [9]
TaO_x, HfO_x, TiO_x	-5 V	±2 V	Wedig et al. (2015) [10]
Ta2O5	+2-3.2 V	+0.45-0.65	Zaffora et al. (2017) [11]
TiO_x	1.5 V	+0.6	Srivastava et al. (2017) [12]
Multilayer Matrix			
Pt/Ta_2O_{5-x}/TaO_{2-x}/Pt	-3 V	-1/+2 V	Lee et al. (2011) [13]
Pt/TiO_x/TiO_y/TiO_x/Pt	-10 V	±1.5 V	Bae et al. (2012) [14]
Pt/Ta_2O_5/HfO_{2-x}/TiN	-10 V	±3-4 V	Yoon et al. (2014) [15]
Pd/Si:Ta_2O_{5-x}/TaO_y/Pd	4-10 V	-1to -1.5 V	Kim et al. (2014) [16]
Pt/Nb-$SrTiO_3$-Sm_2O_3 interface	Forming-free	10 V	Lee et al. (2014) [17]
Pt/HfO_2/Hf/Pt	2.5 V	±1.5 V	Breuer et al. (2015) [18]
Ag/MoO_x/MoS_2/Ag	Forming-free	±0.2 V	Bessonov et al. (2015) [19]
Ta/TaO_x/TiO_2/Ti	Forming-free	±6 V	Wang et al. (2015) [20]
Au/$BaTiO_3$/NiO/Pt	+6 V	±1 V	Li et al. (2016) [21]
Pt/HfOx/HfO2/Pt	+3-10 V	+2-4 V	Cho et al. (2017) [22]
Pt/TiO_x/TaO_x/Pt	Forming-free	+0.5/-0.7 V	**This work**

Table S2| Reduction in the magnitudes of SET (V_{SET}) and RESET (V_{RESET}) voltages with decreasing stopping voltages (V_{STOP}).

$\mathbf{V_{STOP}}$ (V)	$\mathbf{V_{SET}}$ (V)	$\mathbf{V_{RESET}}$ (V)
2.5	0.634	-2.315
2.0	0.574	-1.906
1.5	0.535	-1.548
1.0	0.512	-1.044
0.5	0.500	-0.732

References:

[1] K. Szot, W. Speier, G. Bihlmayer, R. Waser, *Nat. Mater.* **2006**, *5*, 312.

[2] D. H. Kwon, K. M. Kim, J. H. Jang, J. M. Jeon, M. H. Lee, G. H. Kim, X. S. Li, G. S. Park, B. Lee, S. Han, M. Kim, C. S. Hwang, *Nat. Nanotechnol.* **2010**, *5*, 148.

[3] J. P. Strachan, D. B. Strukov, J. Borghetti, J. J. Yang, G. Medeiros-Ribeiro, R. S. Williams, *Nanotechnology* **2011**, *22*, 254015.

[4] J. P. Strachan, G. Medeiros-Ribeiro, J. J. Yang, M. Zhang, F. Miao, I. Goldfarb, M. Holt, V. Rose, R. S. Williams, *Appl. Phys. Lett.* **2011**, *98*, 242114.

[5] D. B. Strukov, F. Alibart, R. S. Williams, *Appl. Phys. A Mater. Sci. Process.* **2012**, *107*, 509.

[6] J. Park, S. Lee, J. Lee, K. Yong, *Adv. Mater.* **2013**, *25*, 6423.

[7] H. Jiang, Q. Xia, *Nanoscale* **2013**, *5*, 3257.

[8] I. Salaoru, A. Khiat, Q. Li, R. Berdan, T. Prodromakis, *Appl. Phys. Lett.* **2013**, *103*, 233513.

[9] J. Hou, S. S. Nonnenmann, W. Qin, D. A. Bonnell, *Adv. Funct. Mater.* **2014**, *24*, 4113.

[10] A. Wedig, M. Luebben, M. Moors, D. Y. Cho, K. Skaja, T. Hasegawa, K. K. Adepalli, B. Yildiz, R. Waser, I. Valov, *Nat. Nanotechnol.* **2015**, *11*, 67.

[11] A. Zaffora, D. Y. Cho, K. S. Lee, F. Di Quarto, R. Waser, M. Santamaria, I. Valov, *Adv. Mater.* **2017**, *29*, 1.

[12] S. Srivastava, J. P. Thomas, N. F. Heinig, K. T. Leung, *ACS Appl. Mater. Interfaces* **2017**, *9*, 36989.

[13] M. J. Lee, C. B. Lee, D. Lee, S. R. Lee, M. Chang, J. H. Hur, Y. B. Kim, C. J. Kim, D. H. Seo, S. Seo, U. I. Chung, I. K. Yoo, K. Kim, *Nat. Mater.* **2011**, *10*, 625.

[14] Y. C. Bae, A. R. Lee, J. B. Lee, J. H. Koo, K. C. Kwon, J. G. Park, H. S. Im, J. P. Hong, *Adv. Funct. Mater.* **2012**, *22*, 709.

[15] J. H. Yoon, S. J. Song, I. H. Yoo, J. Y. Seok, K. J. Yoon, D. E. Kwon, T. H. Park, C. S. Hwang, *Adv. Funct. Mater.* **2014**, *24*, 5086.

[16] S. Kim, S. Choi, J. Lee, W. D. Lu, *ACS Nano* **2014**, *8*, 10262.

[17] S. Lee, A. Sangle, P. Lu, A. Chen, W. Zhang, J. S. Lee, H. Wang, Q. Jia, J. L. Macmanus-driscoll, *Adv. Mater.* **2014**, *26*, 6284.

[18] T. Breuer, A. Siemon, E. Linn, S. Menzel, R. Waser, V. Rana, *Adv. Electron. Mater.* **2015**, *1*, 1500138.

[19] A. A. Bessonov, M. N. Kirikova, D. I. Petukhov, M. Allen, T. Ryhänen, M. J. A. Bailey, *Nat. Mater.* **2015**, *14*, 199.

[20] Y.-F. Wang, Y.-C. Lin, I.-T. Wang, T.-P. Lin, T.-H. Hou, *Sci. Rep.* **2015**, *5*, 10150.

[21] S. Li, X. Wei, Y. Lei, X. Yuan, H. Zeng, *Appl. Surf. Sci.* **2016**, *389*, 977.

[22] D. Y. Cho, M. Luebben, S. Wiefels, K. S. Lee, I. Valov, *ACS Appl. Mater. Interfaces* **2017**, *9*, 19287.